

## Spin-filtering through excited states in double-quantum-dot pumps

Rafael Sánchez,<sup>1</sup> Ernesto Cota,<sup>2</sup> Ramón Aguado,<sup>1</sup> and Gloria Platero<sup>1</sup>

<sup>1</sup>*Instituto de Ciencia de Materiales, CSIC, Cantoblanco, Madrid, 28049, Spain*

<sup>2</sup>*Centro de Ciencias de la Materia Condensada–UNAM, Ensenada, Mexico*

(Received 5 April 2006; published 21 July 2006)

Recently it has been shown that ac-driven double quantum dots can act as spin pumps and spin filters. By calculating the current through the system for each spin polarization, by means of the time evolution of the reduced density matrix in the sequential tunneling regime (Born-Markov approximation), we demonstrate that the spin polarization of the current can be controlled by tuning the parameters (amplitude and frequency) of the ac field. Importantly, the pumped current as a function of the applied frequency presents a series of peaks which are uniquely associated with a definite spin polarization. We discuss how excited states participating in the current allow the system to behave as a bipolar spin filter by tuning the ac frequency and intensity. We also discuss spin relaxation and decoherence effects in the pumped current and show that measuring the width of the current versus frequency peaks allows us to determine the spin decoherence time  $T_2$ .

DOI: [10.1103/PhysRevB.74.035326](https://doi.org/10.1103/PhysRevB.74.035326)

PACS number(s): 73.23.Hk, 73.40.Gk

### I. INTRODUCTION

Production, control, and detection of spin-polarized current through nanostructures (*spintronics*)<sup>1</sup> has become an area of intense activity in the past few years. This is mostly due to the long coherence times of spins, as compared to charge, giving rise to possible applications in quantum information processing. Proposals for generating spin-polarized currents include spin injection by using ferromagnetic metals<sup>2</sup> or magnetic semiconductors.<sup>3</sup> Alternatively, one may use quantum dots (QD's) as spin filters or spin pumps.<sup>4–6,18</sup> In a semiconductor QD, the number of electrons can be controlled via gate voltages, making it an ideal system to study the transport of individual electrons and probe the structure and properties of the discrete energy-level spectrum. Indeed, the spin of an isolated electron in a QD has been proposed as a quantum bit for the transport of quantum information. For QD spin filters, dc transport through few electron states is used to obtain spin-polarized currents which are almost 100% spin-polarized as demonstrated experimentally by Hanson *et al.*<sup>7</sup> following the proposal of Recher *et al.*<sup>8</sup> The basic principle of spin pumps is closely related to that of charge pumps. In a charge pump a dc current is generated by combining ac driving with either the absence of inversion symmetry in the device or a lack of time-reversal symmetry in the ac signal. The range of possible pumps includes turnstiles,<sup>9</sup> adiabatic pumps, or nonadiabatic pumps based on photon-assisted tunneling (PAT).<sup>10,11</sup> In the last few years, the application of ac electric fields in quantum dots has been shown to be very accurate both to control and to modify their transport and electronic properties.<sup>10</sup> For instance, Sun *et al.*<sup>12</sup> have proposed a spin cell based on a double quantum dot, (DQD) driven by microwave radiation in the presence of an external *nonuniform* magnetic field. For strongly correlated electrons in quantum dots in the Kondo regime, the application of an ac potential has been shown to induce decoherence and destroy the Kondo peak.<sup>13,14</sup> An ac potential modifies as well the electron dynamics within single and double quantum dots, and it has been shown that under certain conditions it induces charge localization and destroys the

tunneling, allowing, by tuning the parameters of the ac field, to control the time evolution of the state occupation and therefore the entanglement character of the electronic wave function.<sup>10,15</sup> Regarding the detection of single-spin states in semiconductor quantum dots, this has been achieved<sup>16,17</sup> using quantum point contacts and spin to charge conversion. These studies allow a determination of spin relaxation times on the order of milliseconds.

Recently, we proposed a scheme for realizing *both* spin filtering and spin pumping in an ac-driven DQD (PAT regime), in the Coulomb-blockade transport regime, by tuning the parameters of the ac field.<sup>18</sup> We considered an asymmetric DQD system with one energy state in the left dot and two orbital states in the right dot, allowing each QD to contain up to two electrons. An in-plane magnetic field breaks the spin degeneracy, producing Zeeman splitting. Thus, for the right dot, we can have the following singlet and triplet states, in order of increasing energy:  $|S_0\rangle = \frac{1}{\sqrt{2}}(|\downarrow\uparrow\rangle - |\uparrow\downarrow\rangle)$ ,  $|T_+\rangle = |\uparrow\uparrow^*\rangle$ ,  $|T_0\rangle = \frac{1}{\sqrt{2}}(|\downarrow\uparrow^*\rangle + |\uparrow\downarrow^*\rangle)$ ,  $|T_-\rangle = |\downarrow\downarrow^*\rangle$ , and  $|S_1\rangle = \frac{1}{\sqrt{2}}(|\downarrow\uparrow^*\rangle - |\uparrow\downarrow^*\rangle)$ , where the electrons in the upper level are marked with an asterisk (\*). In our previous work,<sup>18</sup> we considered a basis up to the lowest-energy triplet state  $|T_+\rangle$  and we discussed the conditions for obtaining spin-polarized current from unpolarized leads. Here, we complement these results by adding the remaining excited triplet states which also participate in the pumping process. We find that at a certain frequency of the ac field and in the presence of a uniform magnetic field the double quantum dot acts as a pump of fully spin polarized electrons. Increasing the ac frequency, we show that an inhomogeneous magnetic field is necessary in order to obtain fully spin-polarized current in the reverse direction. Then the system, in such a configuration, acts as a *bipolar* spin filtering just by tuning the ac frequency.

The periodic variation of the gate potentials in our system, consisting of an asymmetric DQD, allows for a net dc current through the device even with no dc voltage applied.<sup>19,20</sup> if the system is driven at frequencies (or subharmonics) corresponding to the energy difference between two time-independent eigenstates related by the intradot tunneling of

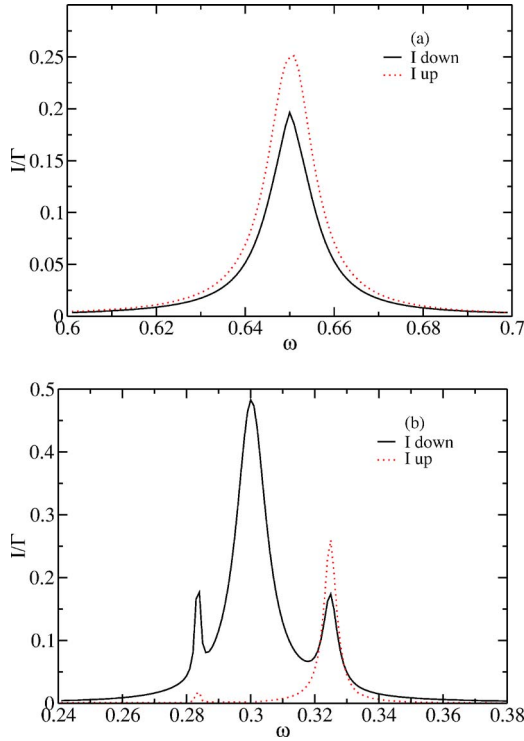


FIG. 1. (Color online) Pumped current as a function of the ac frequency ( $\Delta_L = \Delta_R$ ), for the resonances (a)  $\omega_{T_0\downarrow} = \omega_{T_+\uparrow} \approx 0.65$  and (b)  $\omega_{S_0\downarrow} \approx 0.3$ . At this frequency, the current is fully spin-down polarized. The smaller peaks in (b) are multiphoton satellites of other processes: at  $\omega \approx 0.283$ , the three-photon process corresponding to the resonance between the singlet  $S_0$  in the left dot and the singlet  $S_1$  in the right dot occurs. The two overlapping peaks at  $\omega \approx 0.325$  correspond to two-photon satellites of the resonance in (a). Parameters:  $t_{LR} = 0.005$ ,  $\Gamma = 0.001$ ,  $U_L = 1.0$ ,  $U_R = 1.3$ ,  $\Delta_L = \Delta_R = 0.026$ ,  $\Delta\varepsilon = 0.4$ ,  $J = -0.2$ ,  $\mu_L = \mu_R = 1.31$ ,  $V_{ac} = \omega_{T_+\uparrow}$ .

an electron, this electron become completely delocalized.<sup>21,22</sup> If the left reservoir (chemical potential  $\mu_L$ ) and the right reservoir (chemical potential  $\mu_R$ ) can accept electrons from the right dot (at a rate  $\Gamma_R$ ), the system will then pump electrons from left to right, even when there is no dc bias applied—namely,  $\mu_L = \mu_R$ . Starting from this pumping principle our device has two basic characteristics: (i) If the process involves two-particle states, the pumped current can be completely spin polarized *even if the contact leads are not spin polarized* and (ii) the pumping can occur either through triplet [Fig. 1(a)] or singlet [Figs. 1(b)] states depending on the applied frequency, such that the *degree of spin polarization* can be tuned by means of the ac field. For example, if one drives the system (initially prepared in a state with  $n = n_L + n_R = 3$  electrons:  $|L = \downarrow\uparrow, R = \uparrow\rangle$ ) at a frequency corresponding to the energy difference between the singlets in both dots—namely,  $\omega_{S_0\downarrow} \approx E_{S_0,R} - E_{S_0,L}$  (we consider  $\hbar = e = 1$ )—the electron with spin  $\downarrow$  becomes delocalized in the DQD system. If now the chemical potential for taking  $\downarrow$  ( $\uparrow$ ) electrons out of the right dot is above (below)  $\mu_R$ , a spin-polarized current is generated. The above conditions for the chemical potentials can be achieved by breaking the spin degeneracy through a Zeeman term in each dot:  $\Delta_\alpha = |g| \mu_B B_\alpha$  ( $\alpha = L, R$ ), where  $B_\alpha$  is the

external magnetic field at dot  $\alpha$  (which is applied parallel to the sample in order to minimize orbital effects),  $g$  is the effective  $g$  factor, and  $\mu_B$  is the Bohr magneton. Then, for example, a fully spin-down polarized pump is realized at the frequency  $\omega_{S_0\downarrow}$  through the sequence

$$(\downarrow\uparrow, \uparrow 0) \xrightarrow{ac} (\uparrow, \downarrow\uparrow 0) \xrightarrow{\Gamma_R} (\uparrow, \uparrow 0) \xrightarrow{\Gamma_L} (\downarrow\uparrow, \uparrow 0)$$

or

$$(\downarrow\uparrow, \uparrow 0) \xrightarrow{ac} (\uparrow, \downarrow\uparrow 0) \xrightarrow{\Gamma_L} (\downarrow\uparrow, \downarrow\uparrow 0) \xrightarrow{\Gamma_R} (\downarrow\uparrow, \uparrow 0)$$

which involves singlet states. Increasing the frequency of the ac voltage, the states  $(\downarrow\uparrow, \uparrow 0)$  and  $(\downarrow, T_+)$  are brought into resonance at  $\omega_{T_+\uparrow} \approx E_{T_+,R} - E_{S_0,L}$  and spin-up polarized current flows to the collector from the right quantum dot. However, it can be seen that the state  $(\downarrow\uparrow, \uparrow 0)$  is also in resonance with  $(\uparrow, T_0)$  at the frequency  $\omega_{T_0\downarrow} \approx E_{T_0,R} - E_{S_0,L} = \omega_{T_+\uparrow} + \Delta_R - \Delta_L$ , which coincides with  $\omega_{T_+\uparrow}$  for a homogeneous magnetic field,  $\Delta_R = \Delta_L$ , and this process contributes to spin-down current. Consequently, the current at this frequency is partially spin polarized. This degeneracy, present in the three-electron configuration, is removed if the Zeeman splitting is different in the left and right dots. This could experimentally be achieved either by applying a different magnetic field to each dot or considering quantum dots with different  $g$  factors. In that case,  $\omega_{T_+\uparrow} \neq \omega_{T_0\downarrow}$  and a pure spin-up current is obtained by applying an ac potential with frequency  $\omega_{T_+\uparrow}$ .

In practical implementations of such devices, the effects of spin relaxation and decoherence, characterized, respectively, by times  $T_1$  and  $T_2$ , need to be addressed. The most important source of decoherence in quantum dots is the hyperfine interaction between electron and nuclear spins. Recently, several studies have been reported<sup>23–25</sup> measuring these characteristic times and also  $T_2^*$ , the spin dephasing time for an ensemble of nuclear spins. Decoherence effects are included in our model in a phenomenological way and we give an analytical treatment to explain the numerical results. Interestingly, we find that the decoherence time  $T_2$  can be obtained from the width of the current versus frequency peaks.

This paper is organized as follows: in Sec. II we introduce our model and write the equations for the time evolution of the density matrix. In Sec. III we describe the results obtained for homogeneous and inhomogeneous magnetic field. In Sec. IV we study spin relaxation effects, both numerically and analytically, and discuss the possibility of obtaining the decoherence time  $T_2$  from the width and height of the current versus frequency peaks. We finalize with conclusions and outlook in Sec. V.

## II. THEORETICAL MODEL

Our system consists of an asymmetric DQD connected to two Fermi-liquid leads which are in equilibrium with reservoirs kept at the chemical potentials  $\mu_\alpha$ ,  $\alpha = L, R$ . Using a standard tunneling Hamiltonian approach, we write for the full Hamiltonian  $\mathcal{H}_l + \mathcal{H}_{DQD} + \mathcal{H}_z + \mathcal{H}_T$ , where  $\mathcal{H}_l = \sum_\alpha \sum_{k_\alpha} \sum_{\sigma} \epsilon_{k_\alpha} c_{k_\alpha \sigma}^\dagger c_{k_\alpha \sigma}$  describes the leads and  $\mathcal{H}_{DQD} = \mathcal{H}_{QD}^L$

$+\mathcal{H}_{QD}^R+\mathcal{H}_{L\leftrightarrow R}$  describes the DQD.  $\mathcal{H}_{QD}^L$  and  $\mathcal{H}_{QD}^R$  describe each dot, including the charging energies of the dot electrons. The presence of an external magnetic field is taken into account through the term  $\mathcal{H}_Z=\frac{1}{2}\sum_{\alpha,\sigma,\sigma'}\Delta_\alpha d_{\alpha,\sigma}^\dagger(\sigma_z)_{\sigma\sigma'}d_{\alpha,\sigma'}$ , where  $\Delta_\alpha\equiv g\mu_B B_\alpha$  is the Zeeman splitting of the energy levels of each QD in the presence of an external magnetic field  $\vec{B}_\alpha=(0,0,B_\alpha)$ . The model has been described in detail elsewhere<sup>18</sup> but we include the description here for the sake of clarity. It is assumed that only one orbital in the left dot participates in the spin-polarized pumping process whereas two orbitals in the right dot (energy separation  $\Delta\epsilon$ ) are considered. The isolated left dot is thus modeled as a one-level Anderson impurity,  $\mathcal{H}_{QD}^L=\sum_\sigma E_L^\sigma d_{L\sigma}^\dagger d_{L\sigma}+U_L n_{L\uparrow} n_{L\downarrow}$ , whereas the isolated right dot is modeled as  $\mathcal{H}_{QD}^R=\sum_{i\sigma} E_{Ri}^\sigma d_{Ri\sigma}^\dagger d_{Ri\sigma}+U_R(\sum_i n_{Ri\uparrow} n_{Ri\downarrow}+\sum_{\sigma,\sigma'} n_{R0\sigma} n_{R1\sigma'})+J\mathbf{S}_0\cdot\mathbf{S}_1$ , including the exchange interaction term. The index  $i=0,1$  denotes the two levels. In practice, we take  $E_L^\uparrow=E_{R0}^\uparrow=0$ ,  $E_L^\downarrow=\Delta_L$  and  $E_{R0}^\downarrow=\Delta_R$ , with charging energies  $U_R>U_L$ .  $\mathbf{S}_i=(1/2)\sum_{\sigma\sigma'} d_{Ri\sigma}^\dagger \sigma_{\sigma\sigma'} d_{Ri\sigma'}$  are the spin operators of the two levels. As a consequence of Hund's rule, the intradot exchange  $J$  is ferromagnetic ( $J<0$ ) such that the energy of the singlet  $|S_1\rangle=(1/\sqrt{2})(d_{R0\uparrow}^\dagger d_{R1\downarrow}^\dagger-d_{R0\downarrow}^\dagger d_{R1\uparrow}^\dagger)|0\rangle$  ( $E_{S_1,R}=U_R+\Delta_R+\Delta\epsilon-\frac{3J}{4}$ ) is higher than the energy of the triplets  $|T_+\rangle=d_{R0\uparrow}^\dagger d_{R1\uparrow}^\dagger|0\rangle$ , ( $E_{T_+,R}=U_R+\Delta\epsilon+\frac{J}{4}$ ),  $|T_0\rangle=(1/\sqrt{2})\times(d_{R0\uparrow}^\dagger d_{R1\downarrow}^\dagger+d_{R0\downarrow}^\dagger d_{R1\uparrow}^\dagger)|0\rangle$  ( $E_{T_0,R}=U_R+\Delta_R+\Delta\epsilon+\frac{J}{4}$ ), and  $|T_-\rangle=d_{R0\downarrow}^\dagger d_{R1\downarrow}^\dagger|0\rangle$  ( $E_{T_-,R}=U_R+2\Delta_R+\Delta\epsilon+\frac{J}{4}$ ). As can be seen, due to the Zeeman splitting,  $E_{T_-}>E_{T_0}>E_{T_+}$ . Finally, we consider the case where  $\Delta\epsilon>\Delta_R-J/4$  such that the triplet  $|T_+\rangle$  is higher in energy than the singlet  $|S_0\rangle=(1/\sqrt{2})\times(d_{R0\uparrow}^\dagger d_{R0\downarrow}^\dagger-d_{R0\downarrow}^\dagger d_{R0\uparrow}^\dagger)|0\rangle$  ( $E_{S_0,L(R)}=U_{L(R)}+\Delta_{L(R)}$ ).  $\mathcal{H}_{L\leftrightarrow R}=\sum_{i,\sigma} t_{LR} d_{L\sigma}^\dagger d_{Ri\sigma}+\text{H.c.}$ ) describes interdot tunneling. The tunneling between leads and each QD is described by the perturbation  $\mathcal{H}_T=\sum_{k,L,\sigma} V_L(c_{kL\sigma}^\dagger d_{L\sigma}+\text{H.c.})+\sum_{i,k,R,\sigma} V_R(c_{kR\sigma}^\dagger d_{Ri\sigma}+\text{H.c.})$ . In addition we consider an external ac field acting on the dots, such that the single-particle energy levels become time dependent:

$$E_{L(R)}^\sigma \rightarrow E_{L(R)}^\sigma(t) = E_{L(R)}^\sigma \pm \frac{V_{ac}}{2} \cos \omega t, \quad (1)$$

where  $\sigma=\uparrow,\downarrow$  and  $V_{ac}$  and  $\omega$  are the amplitude and frequency, respectively, of the applied field. We have considered a basis of 40 states in the particle number representation which are obtained under these conditions, considering up to two electrons in each QD. To study the dynamics of a system connected to reservoirs one can consider the reduced density matrix (RDM) operator,  $\hat{\rho}=\text{tr}_R \hat{\chi}$ , where one traces all the reservoir states in the complete density operator of the system,  $\hat{\chi}$ . The evolution of the system will be given by the Liouville equation  $\frac{d\hat{\rho}(t)}{dt}=-i[\hat{H}(t),\hat{\rho}(t)]$ . Assuming the Markov approximation,<sup>26</sup> we obtain the master equation, written as

$$\begin{aligned} \dot{\rho}(t)_{m'm} = & -i\omega_{m'm}(t)\rho_{m'm}(t) - i[\hat{H}_{L\leftrightarrow R},\hat{\rho}(t)]_{m'm} \\ & + \left( \sum_{k\neq m} \Gamma_{mk}\rho_{kk}(t) - \sum_{k\neq m} \Gamma_{km}\rho_{mm}(t) \right) \delta_{m'm} \\ & - \gamma_{m'm}\rho_{m'm}(t)(1-\delta_{m'm}), \end{aligned} \quad (2)$$

where  $\omega_{m'm}(t)=E_{m'}(t)-E_m(t)$  is the energy difference between the states  $|m\rangle$  and  $|m'\rangle$  of the isolated DQD,  $\Gamma_{mk}$  are the transition rates for electrons tunneling through the leads, from state  $|k\rangle$  to state  $|m\rangle$ , and  $\gamma_{m'm}$  describes the decoherence of the DQD states due to the interaction with the reservoir. This decoherence rate is related with the transition rates by  $\text{Re}\gamma_{m'm}=\frac{1}{2}(\sum_{k\neq m'}\Gamma_{km'}+\sum_{k\neq m}\Gamma_{km})$ .

Neglecting the influence of the ac field on tunneling processes through the leads, one can calculate these rates by the Fermi golden rule approximation

$$\Gamma_{mn} = \sum_l \Gamma_l (f(\omega_{mn}-\mu_l)\delta_{N_m N_n+1} + [1-f(\omega_{nm}-\mu_l)]\delta_{N_m N_n-1}), \quad (3)$$

where  $\Gamma_l=2\pi\mathcal{D}_l|V_l|^2$ ,  $l=L,R$ , are the tunneling rates for each lead. It is assumed that the density of states in both leads,  $\mathcal{D}_{L,R}$ , and the tunneling couplings  $V_{L,R}$  are energy independent.  $N_k$  is the number of electrons in the system when it is in state  $|k\rangle$ .

We include spin relaxation and decoherence phenomenologically in the corresponding elements of the equation for the RDM. Relaxation processes are described by the spin relaxation time  $T_1=(W_{\uparrow\downarrow}+W_{\downarrow\uparrow})^{-1}$ ; where  $W_{\uparrow\downarrow}$  and  $W_{\downarrow\uparrow}$  are spin-flip relaxation rates fulfilling a detailed balance:  $W_{\uparrow\downarrow}=\exp(-\Delta_z/k_B T)W_{\downarrow\uparrow}$ ; where  $k_B$  is the Boltzmann constant and  $T$  the temperature. A lower bound for the spin relaxation time  $T_1$  on the order of  $\mu\text{s}$  at  $B\approx 0-2T$  was obtained by Fujisawa *et al.*<sup>27</sup> Recently a value of  $T_1=2.58$  ms with a field  $B=0.02$  T was measured<sup>17</sup> for a single QD using a tunnel-rate-selective readout method. In the following, we focus on zero-temperature results such that  $W_{\uparrow\downarrow}=0$  and thus  $T_1=W_{\downarrow\uparrow}^{-1}$ .  $T_2$  is the spin decoherence time—i.e., the time over which a superposition of opposite spin states of a single electron remains coherent. Recently, Golovach, Khaetskii, and Loss<sup>28</sup> obtained that  $T_2=2T_1$  for spin decoherence induced by a spin-orbit interaction. This time can be affected by spin relaxation and by spin dephasing time  $T_2^*$ —i.e., the spin decoherence time for an ensemble of spins. For processes involving hyperfine interactions between electrons and nuclear spins, Petta *et al.*<sup>25</sup> have obtained  $T_2^*\approx 10$  ns from singlet-triplet spin relaxation studies in a DQD. Here we consider two cases  $T_2^*=0.1T_1$  and  $T_2^*=0.001T_1$ .

In practice, we integrate numerically the dynamics of the RDM in the chosen basis. In particular, all the results shown in the next paragraphs are obtained by letting the system evolve from the initial state  $|\uparrow\downarrow,\uparrow\rangle$  until a stationary state is reached. The dynamical behavior of the system is governed by rates which depend on the electrochemical potentials of the corresponding transitions.

We do not include second-order processes such as cotunneling. The current from the right dot to the right contact is given by  $I_{L\rightarrow R}(t)=\Gamma_R\sum_s \rho_{ss}(t)$ , with a similar expression for  $I_{R\rightarrow L}$ . Here, the states  $|s\rangle$  are such that the right dot is occupied.

### III. RESULTS

We analyze the current through an ac-driven double quantum dot, with  $V_{ac}$  and  $\omega$  the amplitude and frequency of the



ac field, weakly coupled to the external leads, in the presence of a magnetic field which induces a spin splitting  $\Delta_z$  in the discrete states of each dot. We assume the ground state in each dot to be the one with spin up. The model that we propose is of general application; i.e., it is valid for both small or large interdot coupling. In particular we show results for a configuration where the coupling of the dots with the leads is weak and symmetric,  $\Gamma_{L,R}=0.001$ , the hopping between the dots is  $t_{LR}=0.005$ , and the charging energy for the left and right dots is  $U_L=1.0$  and  $U_R=1.3$ , respectively. All energy units are in meV. The Zeeman splitting produced by an external homogeneous magnetic field is  $\Delta_L=\Delta_R=0.026$ , corresponding to a magnetic field  $B\approx 1$  T; the exchange constant for the right dot is  $J=-0.2$  and the chemical potentials in the left and right leads are  $\mu_L=\mu_R=1.31$ , respectively. We have considered two levels in the right dot with energy separation  $\Delta\epsilon=0.45$ , and we neglect interdot Coulomb and exchange interactions.

In order to configure the system in a way that electrons can tunnel from the right dot to the right lead only through the transitions  $|\uparrow\downarrow\rangle_R\rightarrow|\uparrow\rangle_R$  we choose the energy parameters so that they satisfy  $U_R<\mu_R<U_R+\Delta_R$ . The energy cost of introducing a second electron with either spin-up or spin-down polarization in the left dot has to be smaller than the chemical potential of the left lead. This is always satisfied if  $\mu_L>U_L+\Delta_L$ . We consider the system to be in the pumping configuration  $\mu_L=\mu_R$  throughout.

Then, if the DQD is initially in the state  $|\uparrow\downarrow,\uparrow\rangle$ , no current will flow through the system unless the ac frequency fits the energy difference between the different states for the left and right dots. For instance,  $|\uparrow\downarrow,\uparrow\rangle\leftrightarrow|\uparrow,\uparrow\downarrow\rangle$  (at  $\omega=\omega_{S_0\downarrow}=U_R-U_L+\Delta_R-\Delta_L$ ),  $|\uparrow\downarrow,\uparrow\rangle\leftrightarrow|\uparrow,T_0\rangle$  (at  $\omega=\omega_{T_0\downarrow}=U_R-U_L+\Delta_R-\Delta_L+\Delta\epsilon+J/4$ ),  $|\uparrow\downarrow,\uparrow\rangle\leftrightarrow|\uparrow,S_1\rangle$  (at  $\omega=\omega_{S_1\downarrow}=U_R-U_L+\Delta_R-\Delta_L+\Delta\epsilon-3J/4$ ), or  $|\uparrow\downarrow,\uparrow\rangle\leftrightarrow|\downarrow,T_+\rangle$  (at  $\omega=\omega_{T_+\uparrow}=U_R-U_L+\Delta\epsilon+J/4$ ). The suffix  $\uparrow$  ( $\downarrow$ ) is used to remark that the interdot tunneling electron has spin-up (-down) polarization. At these frequencies, one electron becomes delocalized undergoing Rabi oscillations with frequency<sup>10</sup>

$$\Omega_R = 2t_{LR}J_\nu\left(\frac{V_{ac}}{\omega}\right), \quad (4)$$

where  $J_\nu$  is the  $\nu$ th-order Bessel function of the first kind and  $\nu$  is the number of photons required for bringing the two states into resonance. It is important to note that the frequencies for transitions involving spin down depend on the difference  $\Delta_R-\Delta_L$  while the one involving spin up does not. As we will show below, this is the main reason for requiring an inhomogeneous magnetic field to obtain spin-up polarized current. One should remark also that the resonance achieved between  $|\uparrow\downarrow,\downarrow\rangle\leftrightarrow|\uparrow,T_-\rangle$  occurs at a photon frequency  $\omega_{T_-\downarrow}=\omega_{T_0\downarrow}$ . Similarly, the resonance  $|\uparrow\downarrow,\downarrow\rangle\leftrightarrow|\downarrow,T_0\rangle$  occurs at  $\omega_{T_0\uparrow}=\omega_{T_+\uparrow}$ .

We have analyzed both homogeneous ( $\Delta_R=\Delta_L$ ) and inhomogeneous ( $\Delta_R\neq\Delta_L$ ) magnetic field cases.

#### A. $\Delta_R=\Delta_L$

As has been discussed above, by tuning the ac frequency a series of spin-polarized current peaks are obtained which

can be identified and related to different interdot resonant processes. If the Zeeman splitting is the same in both dots, interdot tunneling processes involving electrons with different spins, such as, for instance,  $|\uparrow\downarrow,\uparrow\rangle\leftrightarrow|\uparrow,T_0\rangle$  (at  $\omega=\omega_{T_0\downarrow}$ ) and  $|\uparrow\downarrow,\uparrow\rangle\leftrightarrow|\downarrow,T_+\rangle$  (at  $\omega=\omega_{T_+\uparrow}$ ), occur at the same frequency—i.e.,  $\omega_{T_0\downarrow}=\omega_{T_+\uparrow}\approx 0.65$ —and we find two overlapping peaks [Fig. 1(a)]. The current is created through several processes. The dominant ones are  $|\uparrow\downarrow,\uparrow\rangle\leftrightarrow|\uparrow,T_0\rangle\rightarrow\{|\uparrow,\uparrow\rangle\text{ or }|\uparrow\downarrow,T_0\rangle\}\rightarrow|\uparrow\downarrow,\uparrow\rangle$ , which contributes to spin-down current, and  $|\uparrow\downarrow,\uparrow\rangle\leftrightarrow|\downarrow,T_+\rangle\rightarrow\{|\downarrow,\uparrow\rangle\text{ or }|\uparrow\downarrow,T_+\rangle\}\rightarrow|\uparrow\downarrow,\uparrow\rangle$ , which contributes to spin-up current. So, in this case, the current is partially spin-up polarized.

The frequency  $\omega=\omega_{S_0\downarrow}\approx 0.3$  [Fig. 1(b)] corresponds to the one-photon resonance  $|\uparrow\downarrow,\uparrow\rangle\leftrightarrow|\uparrow,\uparrow\downarrow\rangle$ , which is responsible for the large spin-down current peak through the sequence  $|\uparrow\downarrow,\uparrow\rangle\leftrightarrow|\uparrow,\uparrow\downarrow\rangle\rightarrow\{|\uparrow,\uparrow\rangle\text{ or }|\uparrow\downarrow,\uparrow\downarrow\rangle\}\rightarrow|\uparrow\downarrow,\uparrow\rangle$ . These are the only processes that take place at this frequency, so no spin-up current is expected. Two peaks appear in the vicinity of  $\omega_{S_0\downarrow}$ : one at  $\omega=\omega_{S_1\downarrow}/3\approx 0.283$  [which corresponds to the three-photon satellite of resonance  $\omega_{S_1\downarrow}$  (not shown)] and two overlapping peaks at  $\omega\approx 0.325$  [corresponding to the two-photon satellites at  $\omega_{T_0\downarrow}/2=\omega_{T_+\uparrow}/2$ ; see Fig. 1(a)]. The positions of these peaks are completely independent of each other and are determined by the energetics of the system. Thus, we obtain fully spin-down polarized current at  $\omega=\omega_{S_0\downarrow}$ ; i.e., our device acts as a filter for spin-down electrons.

#### B. $\Delta_R\neq\Delta_L$

In order to get a fully spin-up polarized current peak, we consider different Zeeman splittings between both dots. This introduces a separation  $\Delta\omega\approx\frac{\Delta_R-\Delta_L}{n}$  (where  $n$  is the number of photons involved in the resonant transition) between peaks with different spin polarization, as can be seen, for example, by comparing Figs. 1(a) and 2(a).

Similarly, the resonances  $\omega_{T_0\downarrow}$  ( $=\omega_{T_-\downarrow}$ ) are shifted by an amount  $\Delta_R-\Delta_L$  with respect to the resonance at  $\omega_{T_+\uparrow}$  ( $=\omega_{T_0\uparrow}$ ) which is independent of the Zeeman splitting [see Fig. 2(a)]. So we obtain fully spin-up polarized current at  $\omega_{T_+\uparrow}\approx 0.65$  and fully spin-down polarized current at  $\omega_{T_0\downarrow}\approx 0.676$ . In Fig. 2(b), the resonance  $\omega=\omega_{S_0\downarrow}\approx 0.326$  is not well resolved because there are overlapping satellite peaks (at  $\omega=\omega_{T_0\downarrow}/2\approx 0.338$ ,  $\omega=\omega_{T_+\uparrow}/2\approx 0.325$ ,  $\omega=\omega_{S_1\downarrow}/3\approx 0.292$ ). Concretely, we find different processes that contribute to opposite spin polarization currents and depend on the absorption of a different number of photons [therefore, their Rabi frequencies are renormalized with Bessel functions of different orders, Eq. (4)]. It has been shown that for certain ac parameters and sample configurations<sup>19</sup> the height of the current peaks depends on  $\Omega_R$ , which is a nonlinear function of the ac intensity [see Eq. (4)]. Thus, we can manipulate the spin polarization by tuning the intensity of the ac field.

In Fig. 3 we show the current and current polarization as a function of ac-field intensity at  $\omega=\omega_{S_0\downarrow}$ . Here, the spin-up contribution comes from a two-photon resonance ( $\omega$

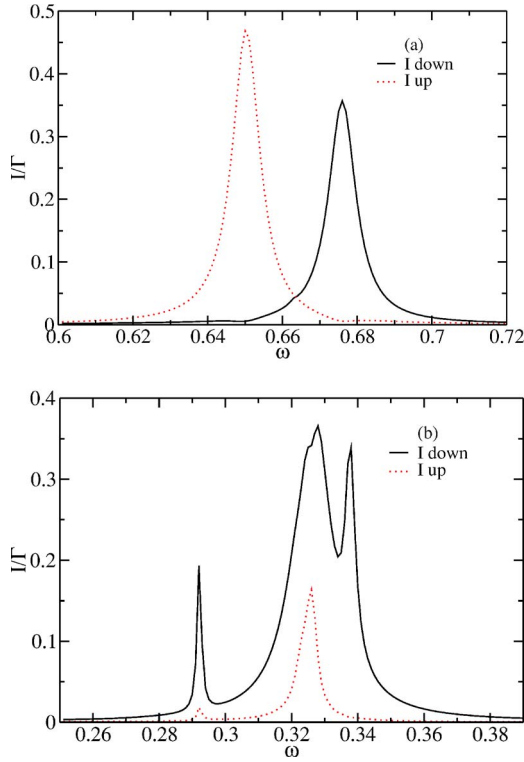


FIG. 2. (Color online) Pumped current as a function of the ac frequency ( $\Delta_L \neq \Delta_R$ ), for the resonances (a)  $\omega_{T_0\uparrow} = \omega_{T_{+\uparrow}} \approx 0.65$  and  $\omega_{T_{0\downarrow}} = \omega_{T_{-\downarrow}} \approx 0.676$  and (b)  $\omega_{S_{0\downarrow}} \approx 0.326$ . The current at the resonance  $\omega = \omega_{S_{0\downarrow}}$  is partially spin-down polarized due to the overlapping satellite peaks (at  $\omega = \omega_{T_{0\downarrow}}/2 \approx 0.338$ ,  $\omega = \omega_{T_{+\uparrow}}/2 \approx 0.325$ ,  $\omega = \omega_{S_{1\downarrow}}/3 \approx 0.292$ ). Parameters:  $t_{LR} = 0.005$ ,  $\Gamma = 0.001$ ,  $U_L = 1.0$ ,  $U_R = 1.3$ ,  $\Delta_L = 0.026$ ,  $\Delta_R = 2\Delta_L$ ,  $\Delta\varepsilon = 0.4$ ,  $J = -0.2$ ,  $V_{ac} = \omega_{T_{+\uparrow}}$ .

$= \omega_{T_{+\uparrow}}/2 \approx 0.325$ ) and, thus, is expected to vanish when  $J_2(\alpha) = 0$  due to the dynamical localization phenomena.<sup>10</sup> Furthermore, for ac intensities such that  $J_1(\alpha) = 0$ , the one-photon resonance  $\omega_{S_{0\downarrow}}$  is quenched and we obtain at this frequency fully spin-up polarized current. Thus, if we tune the ac intensity to the value where the first- (second-) order Bessel function vanishes, we obtain fully spin-up (-down) current. Figure 3(a) shows that at low ac intensities, the contribution of multiphoton processes is small and the  $\omega_{S_{0\downarrow}} \approx 0.326$  resonance corresponding to practically fully spin-down current is clearly resolved.

#### IV. SPIN RELAXATION EFFECTS

It is important to note also that, contrary to the case for spin-down pumping, the pumping of spin-up electrons leaves the double dot in the excited state  $|\downarrow, \uparrow\rangle$ . This makes the spin-up current sensitive to spin relaxation processes. If the spin  $\downarrow$  decays before the next electron enters into the left dot, a spin-down current appears through the cycle

$$(\downarrow, \uparrow) \xrightarrow{ac} (\downarrow, T_+) \xrightarrow{\Gamma_R} (\downarrow, \uparrow) \xrightarrow{W_{\uparrow\downarrow}} (\uparrow, \uparrow) \xrightarrow{\Gamma_L} (\uparrow, \downarrow)$$

and the pumping cycle is no longer 100% spin-up polarized, leading to a reduction of the spin-up current at this frequency.

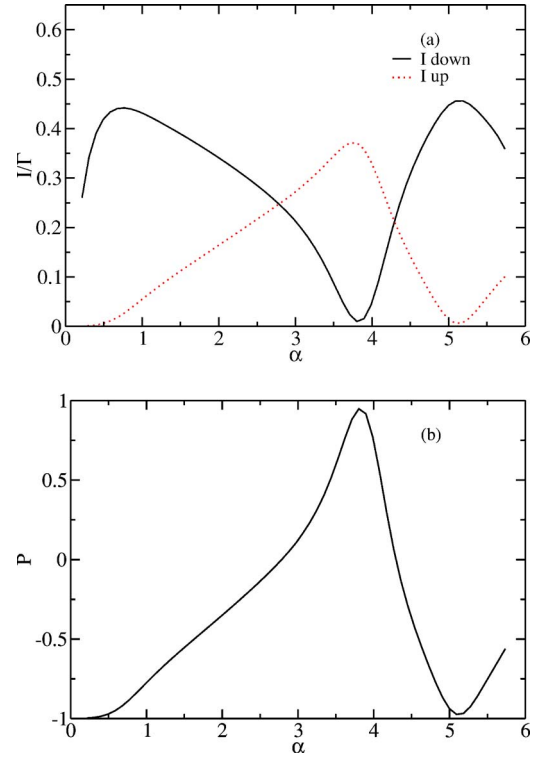


FIG. 3. (Color online) (a) Current and (b) current polarization [defined as  $P = (I_{\uparrow} - I_{\downarrow}) / (I_{\uparrow} + I_{\downarrow})$ ] dependence on the ac field intensity, for  $\omega_{S_{0\downarrow}} = 0.326$ . There is fully spin-up polarization for intensities such that  $J_1(\alpha) = 0$  and fully spin-down-polarization when  $J_2(\alpha) = 0$ . The sample parameters are the same as in Fig. 2.

We include a finite spin-flip relaxation probability,  $W_{\uparrow\downarrow} = 1/T_1 = 5 \times 10^{-6}$  meV and  $T_2^* = 0.1T_1$  and calculate the current at  $\omega_{T_{+\uparrow}} = 0.65$  for different values of the coupling with the contacts,  $\Gamma$ , at  $V_{ac} = 0.14$  meV (Fig. 4). The full widths at half maximum (FWHM) of the current peaks are plotted as a function of  $\Gamma$  in Fig. 5(a) for weak (circles) and strong (squares) ac-field intensity  $V_{ac}$ . In order to minimize nonlinear effects, in Fig. 5(b) we investigate the low-intensity regime ( $V_{ac} = 0.14$ ) where we expect a FWHM dominated by decoherence, for two different values of the spin dephasing time:  $T_2^* = 0.1T_1$  and  $T_2^* = 0.001T_1$ . In every case, we find

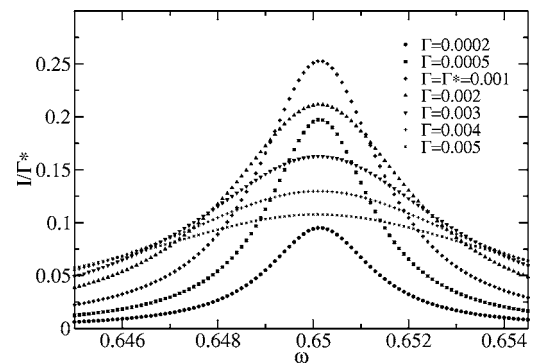


FIG. 4. Pumped current near resonance  $\omega = 0.65$  for different symmetric couplings to the leads.  $\Delta_c^R = \Delta_c^L/0.3$ ,  $W_{\uparrow\downarrow} = 5 \times 10^{-6}$ ,  $V_{ac} = 0.14$ , and  $T_2^* = 0.1T_1$ .

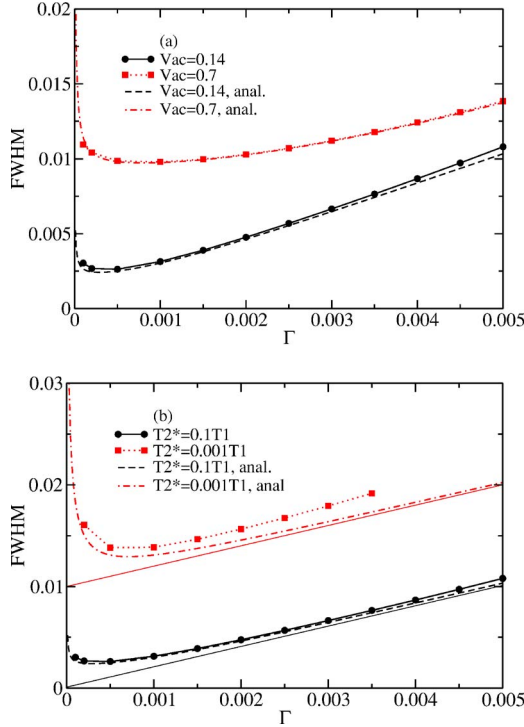


FIG. 5. (Color online) Full width at half maximum of the total current in Fig. 4 as a function of coupling to the leads,  $\Gamma$ , at frequency  $\omega=0.65$  (a) for strong (squares) and weak (circles) field intensities and  $T_2^*=0.1T_1$  and (b) for different spin dephasing times  $T_2^*=0.1T_1$  (circles) and  $T_2^*=0.001T_1$  (squares), for the weak-field intensity case. In both cases, the numerical results are compared to the analytic prediction (dashed lines) given by Eq. (12). (a) In the weak-field case,  $V_{ac}=0.14$ ,  $\Omega_R \approx 0.001$  (circles), we see that for  $\Gamma \gg \Omega_R$ , the curve follows a linear behavior:  $\text{FWHM} \approx 2\gamma = 2(W_{\uparrow\downarrow}/2 + 1/T_2^* + \Gamma)$ . For the high-field intensity case  $V_{ac}=0.7$ ,  $\Omega_R \approx 0.004$  and the same behavior is expected at larger  $\Gamma$ . In (b), for  $T_2^*=0.001T_1$  (squares), we see that the width of the peak is larger than the expected asymptotic behavior for large  $\Gamma$ . This is due to overlapping with the peak at  $\omega_{T_0\downarrow}$ . As discussed in the text, the extrapolation of the asymptotic curves at  $\Gamma=0$  gives the value of  $2(1/2T_1 + 1/T_2^*)$ . Thus, for the case where  $T_2^* \ll T_1$ , this would allow us to estimate the value of the spin dephasing time. In both graphics,  $\Delta_z^R = \Delta_z^L/0.3$ ,  $W_{\uparrow\downarrow} = 1/T_1 = 5 \times 10^{-6}$ .

that for large  $\Gamma$ , the behavior of the FWHM is linear with a slope which approaches 2—i.e.,  $\text{FWHM} \sim 2\Gamma$ —which can be directly related to the decoherence time  $T_2$  as we show below. Thus, experiments along these lines would complement the information about decoherence extracted from other setups.<sup>29,30</sup> As an illustration we present below an analytical treatment which allows us to relate the current peak widths with the spin decoherence time.

### A. Analytical treatment

In the following we present an analytical treatment in the stationary regime of the case discussed above where the influence of spin-flip processes on the spin up current peak coming from the ac-induced resonance between  $|1\rangle = |\uparrow\downarrow, \uparrow\rangle$  and  $|2\rangle = |\downarrow, \uparrow\uparrow^*\rangle$  was numerically obtained.

As discussed in the previous section, at  $\omega = \omega_{T_0\uparrow}$ , these states are brought into resonance and the current, for  $\Delta_R \approx \Delta_L/0.3$ , is fully spin-up polarized. Intermediate states are  $|3\rangle = |\downarrow, \uparrow\rangle$ ,  $|4\rangle = |\uparrow\downarrow, \uparrow\uparrow^*\rangle$ ,  $|5\rangle = |\uparrow, \uparrow\uparrow^*\rangle$ , and  $|6\rangle = |\uparrow, \uparrow\rangle$ . From Refs. 19 and 20 it is known that the dynamics of the system at large time scales is obtained by a time-dependent basis transformation on the density matrix [rotating-wave approximation (RWA)] such that  $\epsilon(t) \rightarrow \epsilon_0 - n\omega$  and  $t_{LR} \rightarrow \tilde{t}_{LR} = (-1)^n J_n(V_{ac}/\omega)t_{LR}$ . The equations of motion for the corresponding reduced density matrix elements in the RWA are

$$\dot{\rho}_1 = -2\tilde{t}_{LR} \text{Im} \rho_{2,1} + \Gamma_L \rho_3 + \Gamma_R \rho_4 + \Gamma_L \rho_6,$$

$$\dot{\rho}_2 = 2\tilde{t}_{LR} \text{Im} \rho_{2,1} - (\Gamma_R + \Gamma_L + W_{\uparrow\downarrow})\rho_2, \quad (5)$$

while for the intermediate states,

$$\dot{\rho}_3 = \Gamma_R \rho_2 - (\Gamma_L + W_{\uparrow\downarrow})\rho_3,$$

$$\dot{\rho}_4 = \Gamma_L \rho_2 - \Gamma_R \rho_4 + \Gamma_L \rho_5,$$

$$\dot{\rho}_5 = W_{\uparrow\downarrow} \rho_2 - (\Gamma_L + \Gamma_R)\rho_5,$$

$$\dot{\rho}_6 = -\Gamma_L \rho_6 + \Gamma_R \rho_5 + W_{\uparrow\downarrow} \rho_3. \quad (6)$$

The equation for the off-diagonal density matrix element is

$$\dot{\rho}_{2,1} = [i(\epsilon_0 - n\omega) + \gamma]\rho_{2,1} + i\tilde{t}_{LR}(\rho_2 - \rho_1), \quad (7)$$

where  $\gamma = 1/T_2$  is the decoherence rate:

$$\gamma = \frac{1}{2}(\Gamma_L + \Gamma_R + W_{\uparrow\downarrow}) + \frac{1}{T_2^*}. \quad (8)$$

This, together with the condition of conservation of probability,  $\sum_i \rho_i = 1$ , gives for the total current (at this frequency), in the stationary regime, an expression which we can write<sup>20</sup> as

$$I = I_0 \frac{W^2}{W^2 + (\epsilon_0 - n\omega)^2}, \quad (9)$$

where  $I_0 = 2\gamma\tilde{t}_{LR}^2/W^2$  is the current maximum and  $W$  is the half width at half maximum:

$$W^2 = \frac{2\gamma\tilde{t}_{LR}^2}{\Gamma_L + \Gamma_R + W_{\uparrow\downarrow}} \left[ \tilde{\Gamma} + \frac{W_{\uparrow\downarrow}}{\Gamma_L + \Gamma_R}(\tilde{\Gamma} - 1) \right] + \gamma^2. \quad (10)$$

Here,  $\tilde{\Gamma} = (\Gamma_L + \Gamma_R)^2 / \Gamma_L \Gamma_R$ . For the symmetric case,  $\Gamma_L = \Gamma_R = \Gamma$  ( $\tilde{\Gamma} = 4$ ) we can rewrite this in terms of the Rabi frequency  $\Omega_R = 2\tilde{t}_{LR}$  as

$$W^2 = \frac{2\gamma\Omega_R^2}{2\Gamma + W_{\uparrow\downarrow}} \left( 1 + \frac{3W_{\uparrow\downarrow}}{8\Gamma} \right) + \gamma^2. \quad (11)$$

In our calculations, we have taken  $W_{\uparrow\downarrow} = 5 \times 10^{-6} \ll \Omega_R, \Gamma$  throughout the range of values considered. Then, Eq. (11) simplifies to

$$W^2 = \frac{\gamma\Omega_R^2}{\Gamma} + \gamma^2. \quad (12)$$

In the limit  $W_{\uparrow\downarrow}, 1/T_2^* \ll \Gamma$ , then  $\gamma \approx \Gamma$ , and we get  $W^2 = \Omega_R^2 + \Gamma^2$  in agreement with previous analytical results.<sup>19,20</sup>

From Eq. (12), we obtain the following asymptotic behaviors.

- (i)  $\Gamma \ll \Omega_R$  (strong interdot tunneling)  $\Rightarrow W^2 \approx \Omega_R^2 \gamma / \Gamma$ .
- (ii)  $\Gamma \gg \Omega_R$  (weak interdot tunneling)  $\Rightarrow W \approx \gamma$ .
- (iii)  $\Gamma \approx \Omega_R \Rightarrow W^2 \approx \gamma_R (\Omega_R + \gamma_R)$ , where  $\gamma_R = \Omega_R + 1/T_2^*$ .

In Fig. 5(a) the FWHM of the spin-up current peak is represented as a function of  $\Gamma$  for the case  $T_2^* = 0.1T_1$  together with the analytical curve (11). For the weak-field case  $V_{ac} = 0.14$  (solid circles) with  $\Omega_R \approx 0.001$ , we see that the predictions of the theory are indeed fulfilled. In particular, in the range  $\Gamma \gg \Omega_R$ , the FWHM as a function of  $\Gamma$  is a straight line with slope 2, as expected (FWHM  $\approx 2\gamma = 2/T_2^* + 1/T_1 + 2\Gamma$ ). This means that a direct measure of the decoherence time for the isolated system,  $T_2^{iso}$ ,  $1/T_2^{iso} = 1/T_2^* + 1/2T_1$ , can be obtained from this linear behavior. From Fig. 5(a) it can be verified that the cases (1) [ $W^2 \approx a + b/(\Gamma T_2^{iso})$ ] and (3) are also reproduced. Besides, it is interesting to mention that from these cases one can get information on the Rabi frequency. The same analysis also holds for the strong field case  $V_{ac} = 0.7$  (solid squares), where  $\Omega_R \approx 0.004$ .

Recently, it has been measured that the spin dephasing time  $T_2^*$  induced by hyperfine interaction is tens of nanoseconds.<sup>24,25</sup> This, together with experimental values for  $T_1$  as long as milliseconds<sup>17</sup> in GaAs quantum dots, such that  $1/T_1 \ll 1/T_2^*$ , would allow us to estimate the spin dephasing time  $T_2^*$  directly from the intersection of the large- $\Gamma$  asymptote with the vertical axis [Fig. 5(b), dotted line].

We note, from Fig. 5(b), that the numerical results differ from the expected analytical curves for the case  $T_2^* = 10^{-3}T_1$  for large  $\Gamma$ . This is because the parameters that contribute to the FWHM ( $\Gamma$  or  $1/T_2^*$ ) are large enough to make the current peak overlap with its neighboring spin-down current peak at  $\omega_{T_0\downarrow}$ . Then, it loses its Lorentzian

shape, mixes its spin polarization, and becomes wider than what is analytically expected. This problem should hold in experimental measurements unless the energy differences between both peaks were large enough so they do not overlap and they can be fitted to a Lorentzian curve. This is the case when  $\Delta_R - \Delta_L \gg 2\gamma$ .

## V. SUMMARY

We have proposed and analyzed a scheme of realizing both spin filtering and spin pumping by using ac-driven double quantum dots coupled to unpolarized leads. Our results demonstrate that the spin polarization of the current can be manipulated (including fully reversing) by tuning the parameters of the ac field. For a homogeneous magnetic field,  $\Delta_L = \Delta_R$ , we obtain spin-down polarized current involving singlet states in both dots. In order to obtain spin-up polarized current, an inhomogeneous magnetic field is required to break the degeneracy in transitions involving triplet states in the right dot. Our results also show, both analytically and numerically, that the width in frequency of the spin-up pumped current gives information about the *spin decoherence time*  $T_2$  and also about the *spin dephasing time*  $T_2^*$  of the isolated double-quantum-dot system. Experiments along these lines would allow us to get information, from transport measurements, on the different mechanisms producing spin decoherence in quantum dots.

We thank J. A. Maytorena for useful discussions. Work supported by Programa de Cooperación Bilateral CSIC-CONACYT, by EU Grant No. HPRN-CT-2000-00144, and by the Ministerio de Ciencia y Tecnología of Spain through Grant No. MAT2002-02465.

- 
- <sup>1</sup>S. A. Wolf, D. D. Awschalom, R. A. Buhrman, J. M. Daughton, S. von Molnar, M. L. Roukes, A. Y. Chtchelkanova, and D. M. Treger, *Science* **294**, 1488 (2001).
  - <sup>2</sup>M. Johnson and R. H. Silsbee, *Phys. Rev. Lett.* **55**, 1790 (1985); F. J. Jedema, A. T. Filip, and B. J. van Wees, *Nature (London)* **410**, 345 (2001).
  - <sup>3</sup>R. Fiederling, M. Keim, G. Reuscher, W. Ossau, G. Schmidt, A. Waag, and L. W. Molenkamp, *Nature (London)* **402**, 787 (1999); Y. Ohno, D. K. Young, B. Beschoten, F. Matsukura, H. Ohno, and D. D. Awschalom, *ibid.* **402**, 790 (1999).
  - <sup>4</sup>E. R. Mucciolo, C. Chamon, and C. M. Marcus, *Phys. Rev. Lett.* **89**, 146802 (2002); Susan K. Watson, R. M. Potok, C. M. Marcus, and V. Umansky, *ibid.* **91**, 258301 (2003); M. G. Vavilov, L. Di Carlo, and C. M. Marcus, *Phys. Rev. B* **71**, 241309(R) (2005).
  - <sup>5</sup>T. Aono, *Phys. Rev. B* **67**, 155303 (2003).
  - <sup>6</sup>E. Cota, R. Aguado, C. E. Creffield, and G. Platero, *Nanotechnology* **14**, 152 (2003).
  - <sup>7</sup>R. Hanson, L. M. K. Vandersypen, L. H. Willems van Beveren, J. M. Elzerman, I. T. Vink, and L. P. Kouwenhoven, *Phys. Rev. B* **70**, 241304(R) (2004).
  - <sup>8</sup>P. Recher, E. V. Sukhorukov, and D. Loss, *Phys. Rev. Lett.* **85**, 1962 (2000).
  - <sup>9</sup>M. Blaauboer and C. M. L. Fricot, *Phys. Rev. B* **71**, 041303(R) (2005).
  - <sup>10</sup>G. Platero and R. Aguado, *Phys. Rep.* **395**, 1 (2004) and references therein.
  - <sup>11</sup>W. G. van der Wiel *et al.*, in *Strongly Correlated Fermions and Bosons in Low-dimensional Disordered Systems*, edited by I. V. Lerner *et al.* (Kluwer Academic, Dordrecht, 2002), pp. 43–68.
  - <sup>12</sup>Qing-feng Sun, Hong Guo, and Jian Wang, *Phys. Rev. Lett.* **90**, 258301 (2003).
  - <sup>13</sup>R. López, R. Aguado, G. Platero, and C. Tejedor, *Phys. Rev. B* **64**, 075319 (2001).
  - <sup>14</sup>J. M. Elzerman, S. de Franceschi, D. Goldhaber-Gordon, W. G. van der Wiel, and L. P. Kouwenhoven, *J. Low Temp. Phys.* **118**, 375 (2000).
  - <sup>15</sup>C. E. Creffield and G. Platero, *Phys. Rev. B* **65**, 113304 (2002); **69**, 165312 (2004).
  - <sup>16</sup>J. M. Elzerman, R. Hanson, L. H. Willems van Beveren, B. Witkamp, L. M. K. Vandersypen, and L. P. Kouwenhoven, *Nature (London)* **430**, 431 (2004).
  - <sup>17</sup>R. Hanson, L. H. Willems van Beveren, I. T. Vink, J. M. Elzerman, W. J. M. Naber, F. H. L. Koppens, L. P. Kouwenhoven, and



- L. M. K. Vandersypen, Phys. Rev. Lett. **94**, 196802 (2005).
- <sup>18</sup>Ernesto Cota, Ramón Aguado, and Gloria Platero, Phys. Rev. Lett. **94**, 107202 (2005).
- <sup>19</sup>C. A. Stafford and N. S. Wingreen, Phys. Rev. Lett. **76**, 1916 (1996).
- <sup>20</sup>B. L. Hazelzet, M. R. Wegewijs, T. H. Stoof, and Yu. V. Nazarov, Phys. Rev. B **63**, 165313 (2001).
- <sup>21</sup>T. H. Oosterkamp *et al.*, Nature (London) **395**, 873 (1998).
- <sup>22</sup>J. R. Petta, A. C. Johnson, C. M. Marcus, M. P. Hanson, and A. C. Gossard, Phys. Rev. Lett. **93**, 186802 (2004).
- <sup>23</sup>K. Ono and S. Tarucha, Phys. Rev. Lett. **92**, 256803 (2004).
- <sup>24</sup>F. H. L. Koppens, J. A. Folk, J. M. Elzerman, R. Hanson, L. H. Willems van Beveren, I. T. Vink, H. P. Tranitz, W. Wegscheider, L. P. Kouwenhoven, and L. M. K. Vandersypen, Science **309**, 1346 (2005).
- <sup>25</sup>J. R. Petta *et al.*, Science **309**, 2180 (2005).
- <sup>26</sup>K. Blum, *Density Matrix Theory and Applications* (Plenum Press, New York, 1996).
- <sup>27</sup>Toshimasa Fujisawa, Yasuhiro Tokura, and Yoshiro Hirayama, Phys. Rev. B **63**, 081304(R) (2001).
- <sup>28</sup>A detailed study of spin relaxation and decoherence in a GaAs quantum dot due to spin-orbit interaction can be found in Vitaly N. Golovach, Alexander Khaetskii, and Daniel Loss, Phys. Rev. Lett. **93**, 016601 (2004).
- <sup>29</sup>Rafael Sánchez, Ernesto Cota, Ramón Aguado, and Gloria Platero, Physica E (Amsterdam), doi: 10.1016/j.physe.2006.03.154 (2006).
- <sup>30</sup>See also Hans-Andreas Engel and Daniel Loss, Phys. Rev. Lett. **86**, 4648 (2001).